

Modeling the Frequency dependence of capacitance in Metal-Insulator-Metal capacitors

R. Karthik^{1#} and A. Akshaykranth¹

ABSTRACT

This paper presents the frequency dependence of capacitance in high-density barrier type anodic TiO₂ metal-insulator-metal (MIM) capacitor. For a capacitance density of 30fF/μm², it is found that increase in anodization voltage influences the capacitance variation with frequency because of change in crystalline and polarization properties of TiO₂. The defect profile is extracted and the polarization is studied using “Electrode polarization” model. The model and measurement results show that anodic TiO₂ is a potential candidate for high quality MIM capacitors for applications with wide operation frequency range.

Keywords: Anodization, Frequency dependant capacitance, MIM capacitor, Polarization.

1. INTRODUCTION

Anodization becomes attractive and efficient deposition method of high-*k* dielectrics for metal-insulator-metal (MIM) capacitors which has been extensively investigated by many authors in recent years [1-5]. With advantages of low structural defects and improved polarization, anodization results low dependence of capacitance with voltage and frequency with low leakage in MIM capacitors which are recommended by International Technology Roadmap for Semiconductors (ITRS) [6]. In particular, frequency dependence of capacitance shows the dependence of structural, dielectric and electrical properties [7]. Frequency dependence of capacitance has been extensively analyzed for various high-*k* dielectrics such as Al₂O₃ [1, 2] and AlTiO_x [8]. However a large dispersion in capacitance is found in AlTiO_x MIM capacitor. This is due to the high defect density and slow time constant of traps in Ti-O_x [8]. But anodic oxidation results a low sensitivity of capacitance with frequency, it is due to crystalline and reduction of defect/traps available at bulk and metal-insulator interface [1].

TiO₂ is an attractive dielectric material with high dielectric constant (80-120) which exists in 3 crystalline phases namely rutile, anatase and brookite. It has been well understood that anodic TiO₂ shows an amorphous-to-crystalline transition at low voltage (~10V) itself [8]. H. Habazaki *et al* have directly proved the crystalline TiO₂ by transmission electron microscopy (TEM) [9]. Various methods have been proposed to deposit TiO₂ such as DC magnetron sputtering [10], and atomic layer deposition [11] to fabricate MIM capacitors. However, frequency dependence of capacitance in TiO₂ - based MIM capacitors has not been studied before. In this letter, we present fabrication of TiO₂ MIM capacitor using anodic oxidation for the first time and a detail study on the influence of anodization voltage in capacitance variation with frequency. The capacitor shows high capacitance density of more than 30fF/μm² at 10 KHz and low dispersion of capacitance with frequency (34% from 1 KHz to 100 KHz and 8% from 100 KHz to 1MHz).

^{#1} Department of Electronics & Communication Engineering, MLR Institute of Technology, Hyderabad, India, *Emails:* karthik.r@mlrinstitutions.ac.in akshaykranth417@gmail.com

2. EXPERIMENTAL PROCEDURE

A bilayer of 15nm Ti on 100nm Al is deposited over 100nm thermally oxidized SiO₂ over Si substrate using electron beam evaporator with tungsten filament at a pressure of 8×10^{-5} mBar. Top Ti film was anodized in a solution of ammonium pentaborate (APB) dissolved in ethylene glycol (20g/l) at various anodization voltages of 10V, 15V and 20V till current density reduces to $1 \mu\text{A}/\text{cm}^2$. Electrolyte solution was prepared by adding 17gm of APB for every 100ml of ethylene glycol [1]. Anodization was done by dipping $\frac{3}{4}$ area of the sample to avoid etching for the bottom electrode. Once cleaned thoroughly by deionized water, a 50nm thick Al top electrode was deposited on the anodized samples using thermal evaporation with the shadow mask area of $\sim 0.61 \text{mm}^2$. Fig. 1 shows the SEM cross section of anodized sample at 20V before top electrode deposition. The capacitance measurement was done using HP4155C semiconductor parameter analyzer.

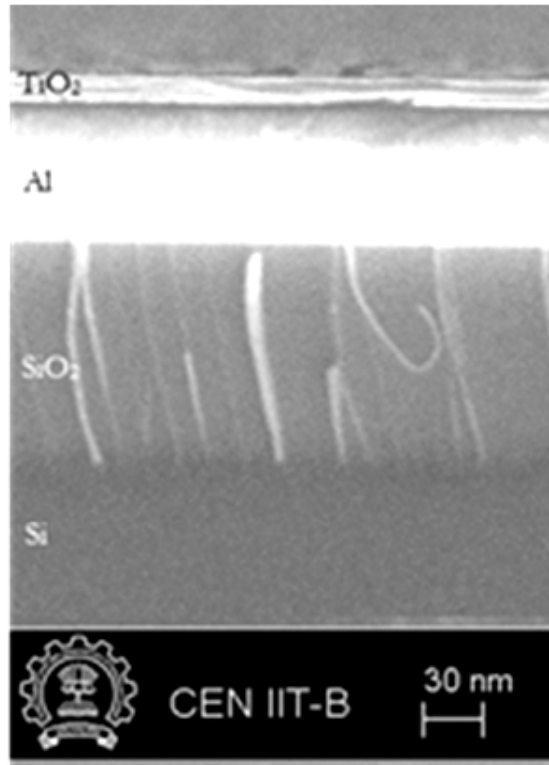


Figure 1: Cross section of anodized sample at anodization voltage of 20V before top electrode deposition

3. MODELING

Fig. 2 shows the measured FDC for various anodization voltages at 25°C. It's found that the capacitance is less sensitive to frequency and improved after 100KHz at higher anodization voltages, this indicate the stronger dipolar polarization is formed. We use Beaumont and Jacobs's electrode polarization model to explain the dispersion of capacitance with frequency which is developed by hopping of carriers and field dependent mobility.

In MIM capacitor, the mobile charges form a double layer near electrodes when AC signal is applied. The double layers are considered as free electrons, injected from electrodes or intrinsic oxygen vacancies [7]. By applying a voltage, the mobile charges are accumulated over a distance L_d from the electrode, called Debye length. This modulation of accumulation region under the AC field is referred as "Electrode polarization". According to Modified Beaumont and Jacobs model [7], the capacitance is

$$C = C_m \left(1 + \frac{A}{\omega^{2n} \tau^{2n}} \right) \quad (1)$$

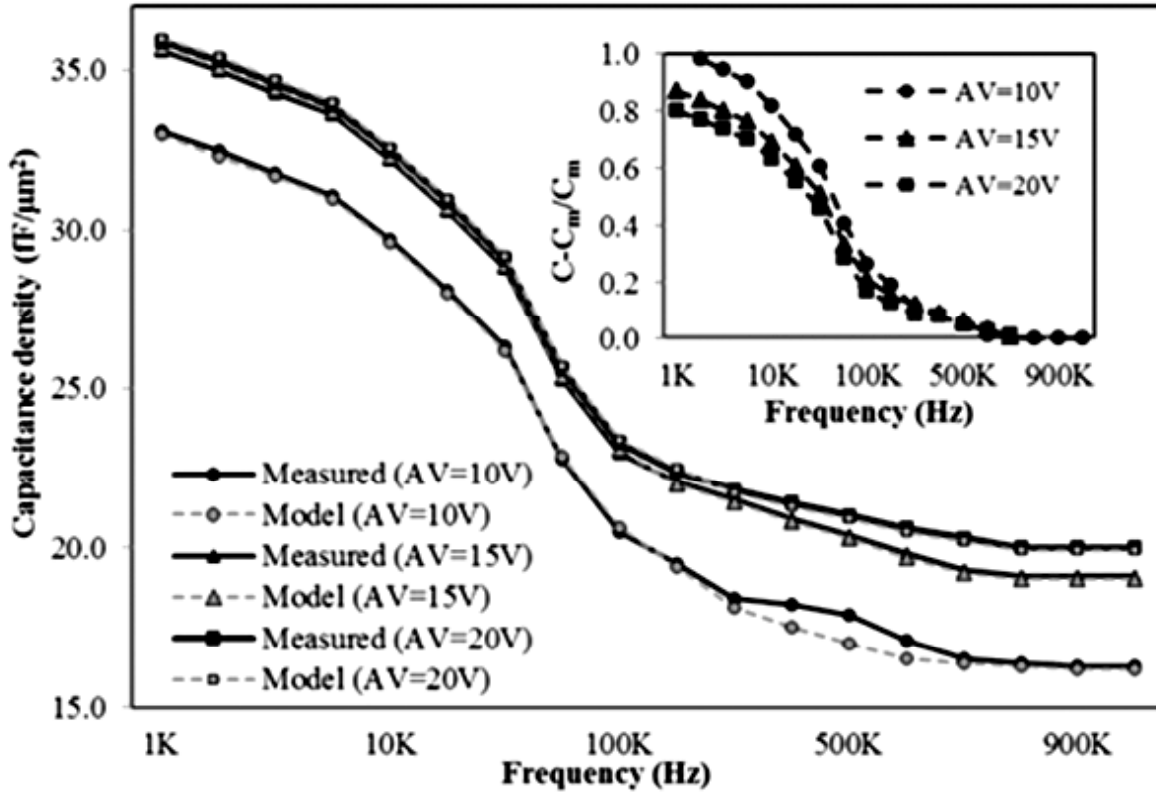


Figure 2: Measured frequency dependent capacitance at various anodization voltages

where C_m is the capacitance for no electrode polarization, expressed as $C_m = \epsilon_0 \epsilon_r S/L$, with top electrode area S and oxide thickness L . In Eq. (1) the slowly varying quadratic second term has $(\omega\tau)^{2n}$ is called Jonscher response, with $0 < n < 1$. ω and τ are angular frequency of AC signal and relaxation time of oxide, respectively. Parameters A and τ are expressed as

$$A = \frac{2}{(2 + \rho)^2} \frac{L}{L_D}, \quad (2)$$

$$\tau = \tau_0 \frac{1}{(2 + \rho)} \frac{L}{L_D}, \quad (3)$$

In equations (2) and (3) intrinsic relaxation time $\tau_0 = \epsilon_0 \epsilon_r / \sigma$ and Debye length $L_D = (\epsilon_0 \epsilon_r k_B T / N_i q^2)^{1/2}$, where N_i is density of intrinsic defects and σ is conductivity of dielectric. ρ is called “blocking parameter” which is a measure of the electrode transparency.

$\rho = \alpha v (L/D) \exp(-E_i / k_B T)$ where α and v are hopping distance and hopping frequency normal to the interface, respectively and D is bulk diffusion coefficient. For strongly injecting contacts, like ohmic contacts, ρ tends to infinity which further gives $A=0$ and $C \approx C_m$. This indicates that space charge is not formed at the metal-dielectric interface. In contrast, when the contact is not injecting any charges, A is very large and ρ is very small. This describes how important is the effect of space charge [7]. We have obtained the parameters of modified Beaumont and Jacobs model [7] by using measured capacitance C and considering $\alpha = 0.5 \text{ nm}$, $v = 10^{12} \text{ Hz}$, $L = 15 \text{ nm}$ and interfacial energy barrier $E_i \approx 0.94 \text{ eV}$ for Al/TiO₂. For this model, with $L_D \approx 0.9 \text{ nm}$, values of τ , N_i and n are obtained for the best fit as anodization voltage is varied. These values are presented in Table. 1. As shown in the table, increasing anodization voltage decreases both defect density N_i and factor n . Hence sensitivity of the TiO₂ MIM capacitor to frequency reduces. Compatibility of the model and measured results is illustrated in Fig. 2.

Table 1
Extracted and Measured parameters

Anodization voltage (Volts)	Measured Capacitance Density at 1V and 10KHz ($fF/\mu m^2$)	Measured conductance at 1V and 1MHz ($\times 10^{-12} S/cm$)	Extracted Model parameters				
			ρ	$\tau(s)$	A	$N_i (cm^{-3})$	n
10	28	2.1	4.3±2	3.52×10^{-5}	0.69±0.2	5.9×10^{18}	0.2 ± 0.1
15	31	0.95	6.0±2	1.07×10^{-5}	0.47±0.2	6.7×10^{17}	0.1 ± 0.1
20	31.5	0.89	8.4±2	1.00×10^{-5}	0.12±0.2	2.9×10^{17}	0.1 ± 0.1

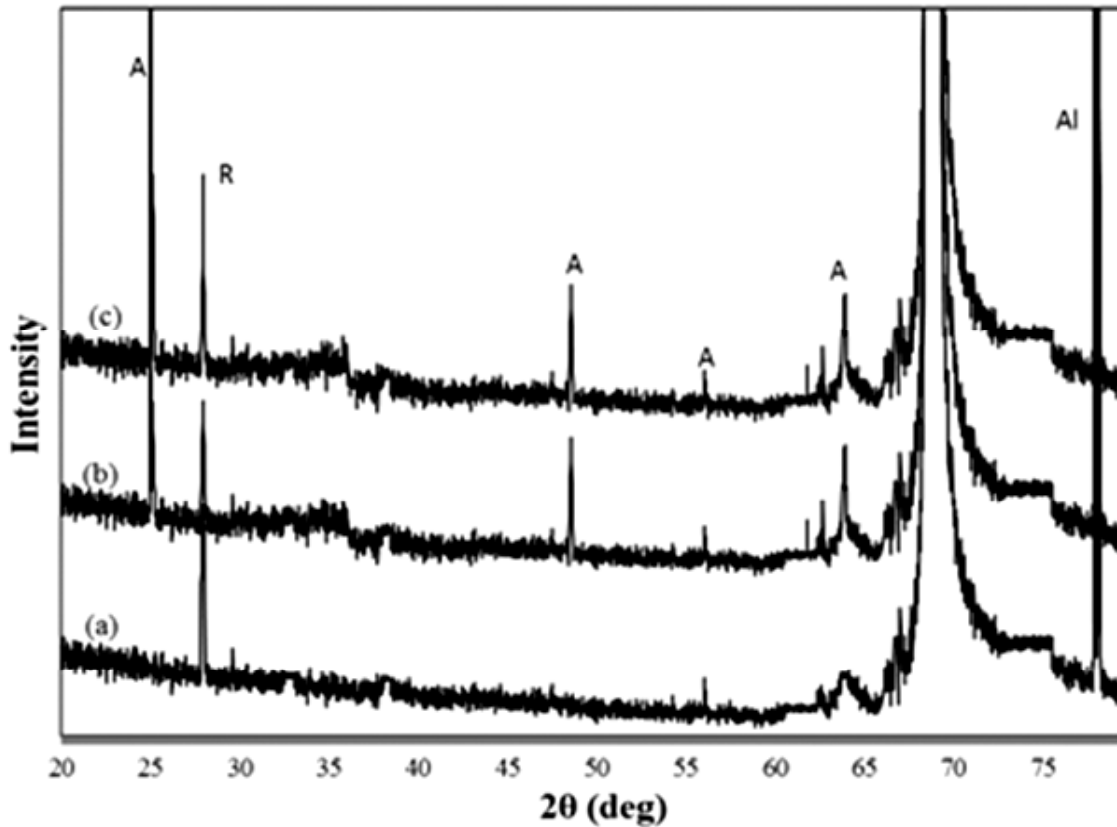


Figure 3: X-Ray Diffraction Spectra of Anodized samples at various anodization voltages (a) 10V (b) 15V (c) 20V (A: Anatase, R: Rutile)

According to L.M. Kosjuk *et al* [12], the second term of the model in Eq. 1 refers the contribution of relaxation polarization in formation of capacitance which is extracted using $(C-C_m)/C_m$ and is shown in the inset of Fig. 2. This slowly varying term decreases in the order from 0.2 to 0.1. This reveals that the relaxation polarization is dominant at lower anodization voltages due to presence of large defects and slow relaxation time. Fig. 3 shows the XRD spectra of three samples, fabricated using different anodization voltages. Spectra shows that the prepared TiO_2 at lower anodization voltage is rutile and partially amorphous (Fig. 3 a). For higher anodization voltages, 15V and 20V, the amorphous state is transferred to crystalline/quasicrystalline state which is confirmed by the peaks for anatase and rutile TiO_2 . At higher anodization voltages, the ionic polarization improves as amorphous state transferred to crystalline with low defect density.

4. CONCLUSION

The experimental results, presented in this paper, demonstrate the anodically grown high-density barrier type TiO_2 MIM capacitor which exhibits reduction in sensitivity of the capacitance with frequency as

anodization voltage increases. The electrode polarization model confirms that the defect profile, polarization, and crystalline properties can be improved at higher anodization voltages. Anodic oxidation of barrier type TiO_2 opens an effective low cost fabrication of high-density MIM capacitors for future RFICs and MMICs.

ACKNOWLEDGMENT

The authors thank Science and Engineering Board (SERB), India for financial support.

REFERENCES

- [1] D. Kannadassan, R. Karthik, M. S. Bhagini, P S Mallick, “Nanostructured Barrier type Anodic oxide Metal-Insulator-Metal capacitors”, *Journal of Nanoelectronics and Optoelectronics*, Vol. 7, pp. 400-404, (2012).
- [2] E. Hourdakis and A. G. Nassiopoulou, “High performance MIM capacitor using anodic alumina dielectric”, *Microelectronics Engineering*, Vol 90, pp.12-16, (2012).
- [3] E Hourdakis, A G Nassiopoulou, “High-Density MIM Capacitors with Porous Anodic Alumina Dielectric”, *IEEE Transactions on Electron Devices*, Vol 57, pp. 2679-2683, (2010).
- [4] Tardy, M. Erouel, A. L. Deman, A. Gagnaire, V. Teodorescu, M. G. Blanchin, B. Canut, A. Barau, and M. Vaharescu, *Microelectronics Reliability*, Vol 47, pp. 372-376, (2007).
- [5] J. T. Lee, B. Parida, J. Choi, and K. Kim, *Journal of Nanoscience and Nanotechnology*, Vol 11, pp. 6389-6394, (2011)
- [6] International Technology Roadmap for Semiconductor (ITRS) 2010, Report on RF and Analog/Mixed Signal design. .
- [7] Gonon, P., Vallée, C., “Modeling of nonlinearities in the capacitance-voltage characteristics of high-k metal-insulator-metal capacitors”, *Applied Physics Letters*, Vol 90, pp. 142906 – 142909, (2007).
- [8] S. B. Chen, C. H. Lai, Albert Chin, J. C. Hsieh, *IEEE Electron Device Letters*, Vol 23, pp. 185-187, (2002).
- [9] H. Habazaki , M. Uozumi , H. Konno , K. Shimizu , P. Skeldon ,G.E. Thompson, “Crystallization of anodic titania on titanium and its alloys”, *Corrosion Science*, Vol 45, pp. 2063–2073, (2003).
- [10] Marius Stamate, Gabriel Lazar, Iulia Lazar, “Dimensional effects observed for the electrical, dielectrical and optical properties of TiO_2 DC magnetron thin films”, *Journal of Material Science: Material Electronics*, Vol. 20, pp. 117-122, (2009).
- [11] M. Seo, S. H. Rha, S. K. Kim, J. H. Han, W. Lee, S. Han, and C. S. Hwang, *Journal of Applied Physics*, Vol 110, pp. 024105-024108, (2011).
- [12] L M Kosjuk, L L Odynets, *Thin Solid Films*, Vol 302, pp. 235-239, (1997).

